

# The impact of a benthic filter feeder: limitations imposed by physical transport of algae to the benthos

William J. Edwards, Chris R. Rehmann, Ellen McDonald, and David A. Culver

**Abstract:** We used an acoustic Doppler profiler to investigate the hydrodynamics of a nearshore site in western Lake Erie, and we incorporated the measured parameters in numerical simulations of phytoplankton consumption by benthic zebra mussels (*Dreissena polymorpha*) to examine the link between pelagic production and benthic filter feeders. Daily-averaged eddy diffusivities varied from  $10^{-5}$  to  $10^{-4}$   $\text{m}^2\cdot\text{s}^{-1}$  at our site. Our simulations demonstrate that diffusivities of this order decrease near-bed algal biomass, while algal biomass in the pelagic remains relatively unaffected. Between 8% and 67% of the algal biomass in the water column could be consumed daily, depending on the shape and magnitude of the diffusivity profile. Correspondingly, in situ vertical biomass profiles showed a near-bed zone of algal depletion, but no impact was observed near the surface. The impact of the zebra mussel in nearshore regions is expected to be stronger than in deeper open water. The flow of algal biomass into the benthos was tightly coupled with turbulent mixing, suggesting that open water algal consumption by zebra mussels is small compared with previously published estimates that ignored vertical turbulent mixing processes.

**Résumé :** Un courantomètre acoustique à effet Doppler nous a permis d'étudier l'hydrodynamique d'un site près de la berge dans la région occidentale du lac Érié; nous avons incorporé les variables mesurées dans des simulations numériques de la consommation de phytoplancton par des moules zébrées (*Dreissena polymorpha*) afin d'examiner le lien qui existe entre la production pélagique et les organismes filtreurs benthiques. Les diffusivités turbulentes moyennes varient de  $10^{-5}$  à  $10^{-4}$   $\text{m}^2\cdot\text{s}^{-1}$  à notre site d'étude. Nos simulations montrent que des diffusivités de cet ordre de grandeur diminuent la biomasse des algues près du coussin de moules, alors que la biomasse des algues dans la zone pélagique demeure relativement inchangée. Entre 8 % et 67 % de la biomasse d'algues présente dans la colonne d'eau peut être consommée à chaque jour, selon la forme et l'importance du profil de diffusivité. De la même façon, les profils verticaux de biomasse en place montrent l'existence d'une zone de densité réduite d'algues près du coussin de moules, mais aucun impact près de la surface. L'effet des moules zébrées dans les régions près des berges doit vraisemblablement être plus grand que dans les eaux ouvertes plus profondes. Le flux de la biomasse des algues vers le benthos est étroitement relié au brassage turbulent, ce qui laisse croire que la consommation d'algues d'eaux libres est faible par rapport aux estimations publiées qui ne tiennent pas compte des processus de brassage turbulent vertical.

[Traduit par la Rédaction]

## Introduction

Despite the investment of substantial resources and effort to evaluate the impact of the zebra mussel (*Dreissena polymorpha*) on aquatic ecosystems, a number of issues remain largely unresolved. The zebra mussel was introduced into the Great Lakes in the late 1980s. Neither the zebra

mussel's direct impact on Great Lakes phytoplankton and zooplankton community dynamics nor its indirect effect on fish community stability is well understood. As their benthic habitat and lack of mobility limit their access to food, zebra mussels depend on transport mechanisms such as settling (algal sinking), turbulent vertical transport, horizontal advection, and resuspension to bring food to them. Thus, any eval-

Received 27 August 2003. Accepted 21 October 2004. Published on the NRC Research Press Web site at <http://cjfas.nrc.ca> on 10 March 2005.  
J17718

**W.J. Edwards.**<sup>1</sup> Department of Biology, Niagara University, Niagara University, NY 14109, USA.

**C.R. Rehmann.** Department of Civil, Construction, and Environmental Engineering, Iowa State University, 374 Town Engineering Building, Ames, IA 50011, USA.

**E. McDonald.**<sup>2</sup> Department of Civil and Environmental Engineering and Geodetic Sciences, The Ohio State University, 2070 Neil Ave., Columbus, OH 43210, USA.

**D.A. Culver.** Department of Evolution, Ecology and Organismal Biology, The Ohio State University, 1315 Kinnear Road, Columbus, OH 43212, USA.

<sup>1</sup>Corresponding author (e-mail: [wje@niagara.edu](mailto:wje@niagara.edu)).

<sup>2</sup>Present address: 1602 Park Ridge Terrace, Arlington, TX 76012, USA.

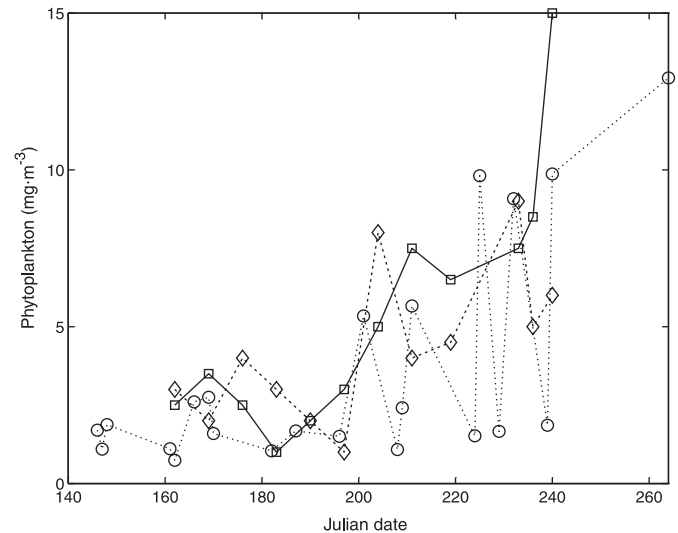
uation of the impact of zebra mussels on the phytoplankton community must be based on a fundamental understanding of both phytoplankton dynamics (changes in population size owing to mortality and reproduction) and physical dynamics (transport throughout the water column owing to turbulent mixing, advection, swimming, or settling) within the system. We use field measurements to investigate the mixing and parameterize a mathematical model of phytoplankton transport resulting from turbulent mixing as a contribution to the understanding of the dynamics of zebra mussel – algae interactions.

While the zebra mussel represents a new and insatiable consumer of algae, its filtering ability has not completely overwhelmed phytoplankton production, in part because algal consumption rates are limited by the rate of delivery of algae to the bottom. Using estimates of mussel population densities and filtering rates, other researchers have speculated that zebra mussels could strip the entire Lake Erie western basin of algae in less than 1 day, or even upwards of 18 times per day (MacIsaac et al. 1992; Bunt et al. 1993; Makarewicz et al. 1999). However, although phytoplankton abundances are now lower and cyanobacteria blooms less frequent than they were prior to 1988, the algal seasonal succession patterns have persisted (Wu and Culver 1991) (Fig. 1). These studies of zebra mussel feeding rates have been based on laboratory work using well-mixed tanks rather than realistic field conditions taking into account the algal delivery rates to the lake bottom and mussels' repeated filtering of the same water (Yu and Culver 1999). In addition, recent research indicates a strong correlation between mussel grazing and hydrodynamic forcing (MacIsaac et al. 1999).

Neglecting the effects of physical forcing in models of trophic dynamics of the Lake Erie ecosystem limits the models' appropriateness both as management tools and as a means to further our basic understanding of lake ecosystems. For example, western Lake Erie is commonly described as completely mixed, and estimates of zebra mussel grazing are based on this assumption (e.g., MacIsaac et al. 1992). Despite the lack of a seasonal thermocline, this assumption is unfounded. Further, marine ecologists have begun quantifying the relationship of fluid mechanics and benthic filter feeders. For example, Muschenheim (1987) studied the feeding ecology of a marine polychaete and concluded that most food is transported horizontally in the low-flow water near the bottom (concentration boundary layer). Vertically settling seston becomes potential food when it enters this boundary layer, but a strong concentration gradient develops with a localized depletion zone near the bed when the filter-feeding organisms remove seston faster than it is replaced. Other researchers have also found a decrease in phytoplankton concentration near marine benthic filter feeders in the field (Frechette and Bourget 1985a; Peterson and Black 1987; Peterson and Beal 1989) and in laboratory experiments (Wright et al. 1982; Wildish and Kristmanson 1984). Vertical feeding height (e.g., height above the bottom) attained by an organism (Jumars and Nowell 1984; Monismith et al. 1990) can thus determine the quantity and quality of its food supply and its rate of growth (Frechette and Bourget 1985b; Frechette et al. 1989).

These marine intertidal zones have long fetches and large tidal fluxes providing more constant and much larger turbu-

**Fig. 1.** Seasonal patterns of algal biomass (wet weight from calculated volumes) before (1988, squares) and after (1989, diamonds; 1998, circles) zebra mussels (*Dreissena polymorpha*) became abundant in Lake Erie. Data from 1988 and 1989 (Wu and Culver 1991) are from weekly 3-m integrated water samples (cf. Wu and Culver (1991) for complete methodology). Data from 1998 are from the Lake Erie Plankton Abundance Survey (Ohio Division of Wildlife) and are averages of 20 weekly 3-m integrated water samples taken from 20 western basin stations.



lent energy inputs than those available in lakes such as Lake Erie. MacIsaac et al. (1992, 1999) found algal depletion in the concentration boundary layer (1.5 m thick) over zebra mussel beds in the western basin of Lake Erie, suggesting that algal delivery in large lakes may also be impacted by vertical mixing. Because mixing processes in lakes are less constant and weaker than their marine counterparts, we hypothesize that the availability of food for the benthic filter feeders, such as the zebra mussel, is even more limited by vertical mixing caused by differential flow or shear within the boundary layer than that demonstrated for marine systems.

Zebra mussels represent a large benthic biomass in western Lake Erie (150 g dry soft tissue·m<sup>-2</sup> at our sampling site in 1995) and excrete large amounts of ammonia and phosphate (Arnott and Vanni 1996; James et al. 1997). At the same time, returning these nutrients to the euphotic zone also requires a mass transport mechanism. Therefore, understanding the role of nutrient and phytoplankton transport in the Lake Erie ecosystem requires identifying and quantifying the important physical, biological, and chemical processes controlling that transport.

We carried out a series of field experiments in the shallow western basin (mean depth = 7 m) of Lake Erie to evaluate shear velocity and estimate eddy diffusivity, measures of vertical mixing intensity. We then used these vertical mixing estimates in a series of simulations to determine the impact of the hydrodynamic forcing on the delivery of algae to the benthos. Finally, we tested these simulations by comparing the results with observed vertical algal distributions and estimating algal turnover rates corresponding to our simulations.

## Materials and methods

### Models

The abundance of algae in the concentration boundary layer depends on the algal settling rate, horizontal advection of phytoplankton, turbulent mixing above the mussel bed, the clearance rate of the zebra mussels, and external sources and sinks resulting from phytoplankton production and grazing by other organisms such as zooplankton (Cloern 1991; Lucas et al. 1999). The interaction of these physical and biological processes ultimately determines how much phytoplankton will be available to the zebra mussels at the bed. In this paper, we have neglected horizontal advection of phytoplankton to compare with earlier zebra mussel consumption estimates (MacIsaac et al. 1992, 1999; Bunt et al. 1993).

### Finite mixing model

Under the above conditions, the effects of vertical mixing, settling, production, and zebra mussel consumption on the phytoplankton biomass can be modeled with a one-dimensional advection–diffusion equation (Cloern 1991):

$$(1) \quad \frac{\partial F}{\partial t} - w_s \frac{\partial F}{\partial z} = \frac{\partial}{\partial z} \left( K \frac{\partial F}{\partial z} \right) + \mu F$$

where  $F$  is the concentration of the phytoplankton,  $t$  is time,  $w_s$  is the settling velocity of the phytoplankton (positive downward),  $z$  is the vertical coordinate,  $K$  is the vertical eddy diffusivity, and  $\mu$  is the phytoplankton turnover rate. The boundary conditions in turn involve the total flux (vertical transport) of phytoplankton. At the water surface ( $z = H$ ), there is no flux and hence no loss or gain of phytoplankton.

$$(2) \quad -w_s F - K \frac{\partial F}{\partial z} = 0 \quad \text{at } z = H$$

At the bottom ( $z = 0$ ), the phytoplankton flux equals the consumption rate of the zebra mussels (Frechette et al. 1989):

$$(3) \quad -w_s F - K \frac{\partial F}{\partial z} = -\alpha F \quad \text{at } z = 0$$

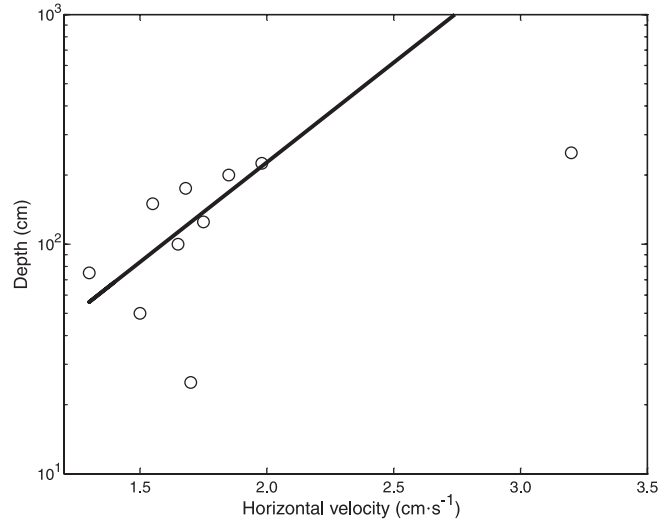
where  $\alpha$  is the clearance rate of the mussels and  $\alpha F$  (evaluated at the bottom) is the algal consumption rate. For initial conditions, we use a uniform algal distribution with depth.

Before solving the system defined by eqs. 1–3, we specify values for the parameters. We used a settling velocity, the rate of algal sinking, of  $1 \text{ m}\cdot\text{day}^{-1}$  (Hutchinson 1967) and a zebra mussel clearance rate  $\alpha = 25 \text{ m}^3\cdot\text{m}^{-2}\cdot\text{day}^{-1}$  (see Discussion). The phytoplankton turnover rate  $\mu$  was weighted according to a typical western basin light penetration curve, with a 10% light penetration point corresponding to 2 m beneath the surface. We estimated the eddy diffusivity assuming rough, turbulent flow, which can be described by a logarithmic velocity profile (Hinze 1975):

$$(4) \quad u = \frac{u_*}{\kappa} \ln \left( \frac{z}{z_0} \right)$$

where  $u = \sqrt{\tau_0/\rho}$  is the shear velocity,  $\tau_0$  is the shear stress on the bed,  $\rho$  is the water density,  $\kappa = 0.4$  is the von Kármán constant, and  $z_0$  is a length scale related to the bottom roughness. This assumption holds true above any bed with rough

**Fig. 2.** Regression fit of time-averaged horizontal velocities versus  $\ln z$  used to estimate  $u_*$ , the shear velocity, and  $z_0$ , the roughness length, for 12 September 1995. The theoretical distribution of the logarithm of depth versus velocities above a bed is linear, necessitating the use of a linear fit in all profiles. This fit is for one 20-min period ( $r^2 = 0.75$ ).



turbulent flow, as in Lake Erie (Chriss and Caldwell 1982; Bedford and Abdelrhman 1987). Estimates of  $u_*$  and  $z_0$  can be obtained by measuring the velocity at a series of points above the bed. When the horizontal component of velocity is plotted against the natural logarithm of the distance above the bottom (eq. 4) (e.g., Fig. 2),  $u_*$  and  $z_0$  can be computed from the slope and intercept, respectively. We assume that the turbulent diffusivity of phytoplankton is equal to that of momentum and that the mixing is due to the shear on the bed. Then the diffusivity has a parabolic distribution with depth (Fischer et al. 1979, p. 106):

$$(5) \quad K = \kappa u_* z \left( 1 - \frac{z}{H} \right)$$

for which the depth-averaged diffusivity is

$$(6) \quad K_{\text{avg}} = \frac{\kappa}{6} u_* H$$

Both the parabolic and uniform distributions of diffusivity are used in the simulations.

After the parameters were specified, the system (eqs. 1–3) was solved numerically, similar to the approach of Koseff et al. (1993), using the Crank–Nicolson method with central differences for the diffusion terms and an upwind difference for the sinking term. Following Koseff et al. (1993), a small, minimum eddy diffusivity was added to the profile in eq. 5; the minimum was typically 100 times smaller than the depth-averaged diffusivity. This minimum diffusivity prevents the generation of artifacts unrelated to the mixing profiles in the simulation results caused by an artificial barrier to mixing when the diffusivity approaches zero. For the range of parameters relevant for the western basin of Lake Erie, the simulation results are insensitive to the value of the minimum eddy diffusivity. We adopted a fully implicit formulation for the boundary conditions, since spurious oscillations

tions develop when the Crank–Nicolson scheme is used (Douglas 1961). Typical values for the time step and grid spacing were 30 s and 0.035 m, respectively. A set of simulations was run to confirm that the results did not depend on these choices and that they matched analytical solutions for simple cases.

### Well-mixed reactor model

The simulations of the effects of mixing and mussel grazing on algal biomass dynamics using eq. 1 are compared with two previous methods of estimating zebra mussel impact: the well-mixed reactor model and the no-refiltration model. The well-mixed reactor model assumes that the lake is well mixed, i.e., the algal concentration is uniform over the water column. Integrating eq. 1 over the depth yields an equation for the total phytoplankton biomass:  $B = \int_0^H F dz$ ; then in the limit of large eddy diffusivity (and constant  $\mu$  profile), one can show that (e.g., Koseff et al. 1993):

$$(7) \quad \frac{dB}{dt} = B \left( \mu - \frac{\alpha}{H} \right)$$

The solution to eq. 7 is an exponential function in which the growth or decay rate depends on mussel consumption and phytoplankton production:

$$(8) \quad B = B_0 e^{(\mu - \alpha/H)t}$$

where  $B_0$  is the initial algal biomass.

### No-refiltration model

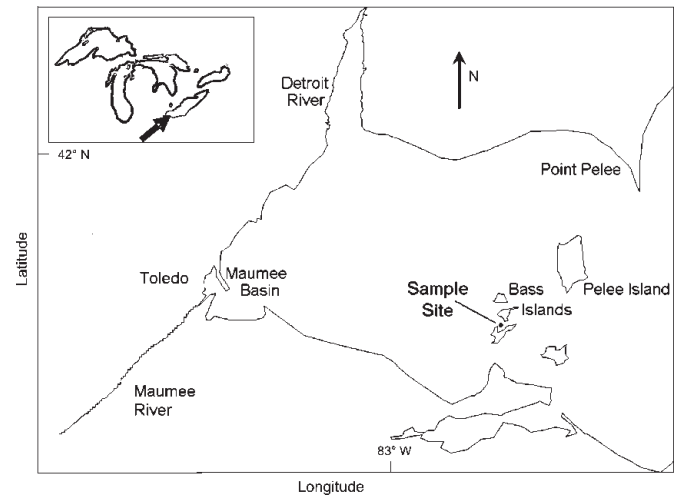
The third and last model, which we call the no-refiltration model, corresponds to combining the pumping rate of mussels with areal estimates of zebra mussel abundance to estimate the amount of water filtered by mussels per square metre per day. It is then assumed that there is no refiltration and that algal concentrations remain constant in water being ingested by the mussels. These assumptions lead to a linear decline of algal biomass (milligrams per square metre) in the water column with time:

$$(9) \quad B = B_0 \left( 1 - \frac{\alpha}{H} t \right)$$

In order for the assumptions of this model to hold true, the lake must remain completely static and algal sinking rates must equal the zebra mussel clearance rate  $\alpha$ . Despite the unusual nature of these assumptions, this model has been used to obtain a theoretical maximum value for mussel impacts on Lake Erie (MacIsaac et al. 1992; Bunt et al. 1993). To include production, the biomass becomes  $B = B_0[(1 + \alpha/\mu H)e^{\mu t} - \alpha/\mu H]$ , which deviates from linear decay except for  $\mu t \ll 1$ . However, this modification is not examined further because eq. 9 is used for comparison with previous work, which did not include production terms.

Whether a water body with zebra mussels is well mixed depends on the speed of the various processes affecting the phytoplankton. For example, Koseff et al. (1993) defined several time scales:  $T_{\text{Graz}} = H/\alpha$  is the time for zebra mussels to filter the equivalent of the water column,  $T_{\text{Mix}} = H^2/K$  is the time for turbulence to mix the water column,  $T_{\text{Sink}} =$

**Fig. 3.** Location of the sampling site between Gibraltar Island and Middle Bass Island in the western basin of Lake Erie. The inset map shows the location within the Great Lakes.



$H/w_s$  is the time for a particle to sink from the surface to the bottom, and  $T_\mu = \mu^{-1}$  is the production time scale. An additional time scale is the duration of the simulation, which was held constant at 24 h. In general, the full model expressed by eqs. 1–3 accounts for all four processes or time scales, while the no-refiltration and well-mixed models do not account for mixing and sinking. (The no-refiltration model does account for sinking. In a way, the well-mixed reactor model also includes sinking, but in the limit of infinite  $K^*$  (high eddy diffusivity), the sinking is unimportant, as we show.)

Comparing systems with different forcing or biological parameters can be facilitated by forming ratios of the time scales. We define the three dimensionless ratios:

$$(10) \quad K^* = \frac{K_{\text{avg}}}{\alpha H} = \frac{T_{\text{Graz}}}{T_{\text{Mix}}}$$

$$(11) \quad w_s^* = \frac{w_s}{\alpha} = \frac{T_{\text{Graz}}}{T_{\text{Sink}}}$$

$$(12) \quad \mu^* = \frac{\mu H}{\alpha} = \frac{T_{\text{Graz}}}{T_\mu}$$

Then, for example, a large value of  $K^*$  implies that turbulence mixes the water column much faster than the zebra mussels can filter the equivalent of the depth. In these terms, one would expect the agreement between the predictions of the full model and the well-mixed model to improve when  $K^*$  becomes large. Furthermore, the nondimensional sinking rate  $w_s^*$  allows comparison between the mussel clearance rate and the sinking rates of the algae. We have varied these nondimensional parameters and presented the effect on algal clearance. The well-mixed reactor is initially set at  $\mu^* = 0$  and  $K^* \rightarrow \infty$  and the no-refiltration model has  $K^* = \mu^* = 0$  and  $w_s^* = 1$ .

### Field methods

Field experiments were conducted in the western basin of Lake Erie (United States) offshore of Gibraltar Island

**Table 1.** Physical parameter variation at our sample site.

Date	Water velocity (cm·s <sup>-1</sup> )	Wind velocity (m·s <sup>-1</sup> )	$z_0$ (cm)	$u_*$ (cm·s <sup>-1</sup> )	$K_{\text{avg}}$ ( $\times 10^{-4}$ m <sup>2</sup> ·s <sup>-1</sup> )
5 June	0.93	2–5 east	22	1.09±0.13	0.36
6 June	1.18	1–2 northeast	13	1.0±0.04	0.33
8 June	1.25	1–2 northeast	7.3	1.32±0.22	0.44
11 June	1.50	2–5 northwest	19	0.80±0.12	0.26
12 June	1.62	2–5 north	11	0.77±0.13	0.25
13 June	1.16	5–10 west	11.2	0.95±0.29	0.31
20 June	1.89	1–2 north	17	0.63±0.17	0.21
22 June	1.57	2–5 northeast	8.5	1.66±0.69	0.55
24 Aug.	4.63	2–5 north	12	0.19±0.12	0.06
25 Aug.	3.08	2–5 northwest	20.4	0.19±0.07	0.06
29 Aug.	1.84	2–5 northeast	13	0.32±0.10	0.10
12 Sept.	2.92	2–5 southwest	12	0.37±0.05	0.12
13 Sept.	4.63	5–10 south	18	0.13±0.12	0.04

**Note:** Mean (24-h) horizontal water velocity at 1 m was measured using the acoustic Doppler profiler, and mean wind velocity and direction were obtained from the Great Lakes Forecasting System (Kelly et al. 1998). The shear velocity  $u_*$  and the roughness length  $z_0$  were calculated by regression using eq. 4 with 20-min time intervals and averaging of the resultant shear velocities over 24 h for each date. Only profiles with  $r^2 > 0.5$  were used to develop a daily average, and only those dates with more than 50% of their profile regressions with  $r^2 > 0.5$  are included above. The mean diffusivity  $K_{\text{avg}}$  was calculated from the shear velocity using eq. 5 for the 5-m water column. The distribution of the shear velocities was examined with histograms and found to be normally distributed; confidence intervals were generated with normally distributed standard error in  $u_*$  above.

(41°40'N, 82°50'W) (Fig. 3). We sampled the bottom 3 m of the 5-m column of water (ranging from 4 to 6 m owing to seiche activities), approximately 50 m from shore, from June until September 1995. The bed consisted of 5- to 10-cm-diameter cobble, with zebra mussels in clumps ranging from 5 to 20 cm in diameter. The zebra mussel dominated the benthic community with between 10 000 and 20 000 mussels·m<sup>-2</sup> and up to 150 g mussel dry soft tissue·m<sup>-2</sup> (Pontius and Culver 2001).

We measured water velocity measurements using a Sontek 3-MHz acoustic Doppler profiler, which was deployed on a steel tripod facing downward, recording the data via a 60-m cable to a shore-based computer. Using the acoustic Doppler profiler, water velocities were measured in 25-cm strata (bins) from the bottom to 3 m above the bottom, with the computer recording time-averaged vertical profiles of the three-dimensional velocity fields every 20 min. We generated a power spectrum (Welch method) from a time series of horizontal velocities from 1 m above the bottom to determine whether the current-forcing processes present at this site were characteristic of the western basin as a whole. We sampled continuously throughout the summer, interrupted only by two electronic failures resulting from lightning strikes on 24 June and 25 August. The horizontal components of velocity were used to estimate  $u_*$  and  $z_0$  and, in turn, the eddy diffusivity using eqs. 4–6. Profiles with good fits (linear regression,  $p < 0.05$ ) were included in a 24-h average diffusivity ( $K_{\text{avg}}$  obtained from eq. 6 with 24-h-averaged  $u_*$  values). Wind speeds corresponding to the sample dates were obtained at 6-h intervals from the Great Lakes Forecasting System (Kelly et al. 1998) to compare with measured mixing parameters. Vertical temperature and oxygen profiles of the whole water column were taken daily (Yellow Springs Instruments dissolved oxygen probe, Yellow Springs, Ohio) to test for significant stratification during the sampling periods.

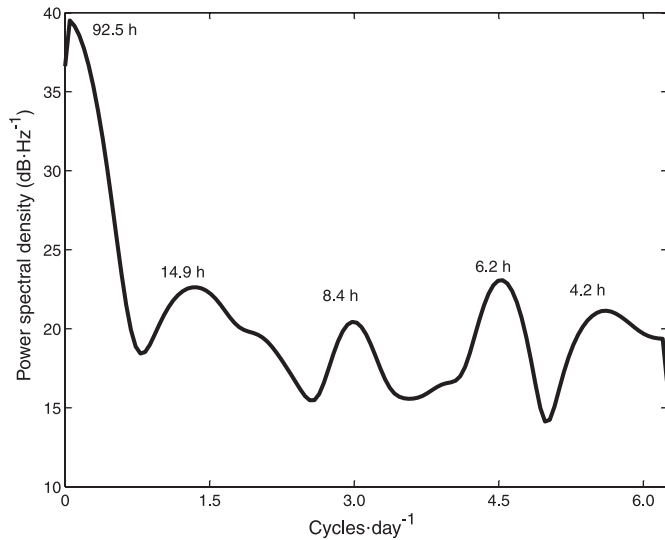
We measured vertical phytoplankton abundance distribution three times per week using two shore-based 10-channel peristaltic pumps. Water was sampled from an apparatus deployed on the acoustic Doppler profiler tripod at fixed depths of 6, 12, 24, 36, 49, 61, 98, 148, 200, and 250 cm above the bed. Tubes from the sampler passed to shore inside an opaque plastic pipe. The tubes were each flushed before sampling by passing twice the tube volume through the tubes prior to collecting samples at only 30 mL·min<sup>-1</sup>. The samples thus represent well the stratum from which each was taken and the 3-L samples used for analysis were integrated over time (~100 min). Phytoplankton samples were preserved using Lugol's fixative and were enumerated using an inverted microscope to produce phytoplankton biomass (milligrams wet mass per litre based on calculated cell biovolumes determined from linear cell dimensions) profiles versus depth for each sample date.

## Results

### Field results

The temperature varied less than 0.1 °C from the surface to the bed during the sampling period. Time-averaged mean horizontal currents ranged from 0.93 to 4.63 cm·s<sup>-1</sup>, while wind velocities from the same periods ranged from 1 to 15 m·s<sup>-1</sup> (Table 1). Although water velocity changes did not appear to correspond to wind speed, the stronger currents tended to coincide with winds from the north. The power spectrum of current velocities 1 m above the bottom was calculated from 10 June 1995 until the first lightning strike on 23 June (Fig. 4) and shows large peaks at 92.5 and 14.9 h, with smaller peaks at 8.4, 6.2, and 4.2 h, with no diel (24-h) signal evident. Using the fit of time-averaged vertical profiles of horizontal velocity versus  $\ln z$  (which have a slope of  $u_*\kappa^{-1}$  and intercept the  $z$  axis at  $z = z_0$ ), we calculated the shear velocities  $u_*$  and the roughness lengths  $z_0$  for each

**Fig. 4.** Power spectrum of horizontal velocities at our sample site at 1 m above the bottom, June 1995. From left to right, peaks correspond to the storm cycle, first-mode seiche, second-mode seiche, third-mode seiche, and a combination of the fourth mode and cross-basin seiches.



date. For example, on 12 September,  $u_* = 0.37 \text{ cm}\cdot\text{s}^{-1}$  and  $z_0 = 12 \text{ cm}$  (Fig. 2). The  $z_0$  varied from 7 cm to as great as 20 cm, whereas individual zebra mussels on the bottom varied in size from 0.1 to 3.0 cm. The  $u_*$  values and the corresponding diffusivities depended primarily on wind direction (Table 1). The roughness Reynolds number  $u_*k_s/\nu$ , where  $k_s = z_0/30$  is the equivalent sand grain roughness of the bed and  $\nu$  is the kinematic viscosity, always exceeded 70, the value required for eq. 4 to be valid (Hinze 1975). The lack of data in the two periods between 22 June and 24 August and again between 24 August and 11 September reflects the periods required for repairs after direct lightning strikes caused electronic failures in the acoustic Doppler profiler. We then estimated the depth-averaged eddy diffusivity using eq. 6. For example, evaluating a daily average  $K$  for 12 September 1995 gave  $K_{\text{avg}} = 1.2 \times 10^{-5} \text{ m}^2\cdot\text{s}^{-1}$ . We thus evaluated  $K_{\text{avg}}$  for each date (Table 1), dropping those dates having weak fits ( $p > 0.05$ ).

Algal biomass varied widely with depth in June and July 1995 (Julian days 92–152; Fig. 5, solid line), with values from samples near the benthos (i.e., zebra mussels) being very low, while farther away, biomass increased exponentially above the bed (nonlinear regression,  $p < 0.01$ ). During August and September, a different trend was apparent, although the variance was large in these samples (Julian days 174–200; Fig. 5, dashed line). Examination of the taxonomic composition in the algae samples indicated that phytoplankton biomass near the bottom was dominated by the cyanobacterium *Microcystis* (e.g., 81% of the algal biovolume in the August 98 cm sample), a vertically migrating (buoyant) species often rejected by zebra mussels (L. Babcock-Jackson, Chemical Abstracts Service, P.O. Box 3012, Columbus, OH 43210, USA, personal communication).

**Simulation results**

Simulations solving eq. 1 indicated less algal consumption than predicted by the well-mixed and no-refiltration ap-

**Fig. 5.** Algal biomass (wet mass from calculated volumes) distributions for early and late summer versus depth above bed at a single site in western Lake Erie. The solid line indicates profiles before 1 August 1995 (mean of five profiles) and the dashed line is after 21 August 1995 until 15 September 1995 (mean of four profiles). The horizontal bars indicate standard deviation around the mean profile.

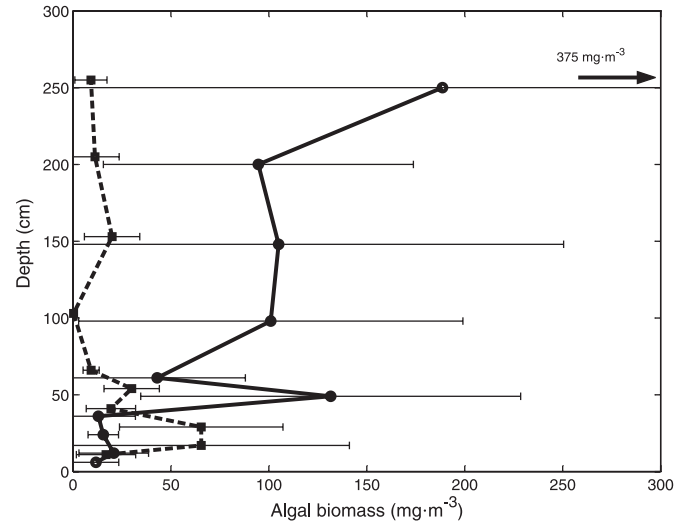
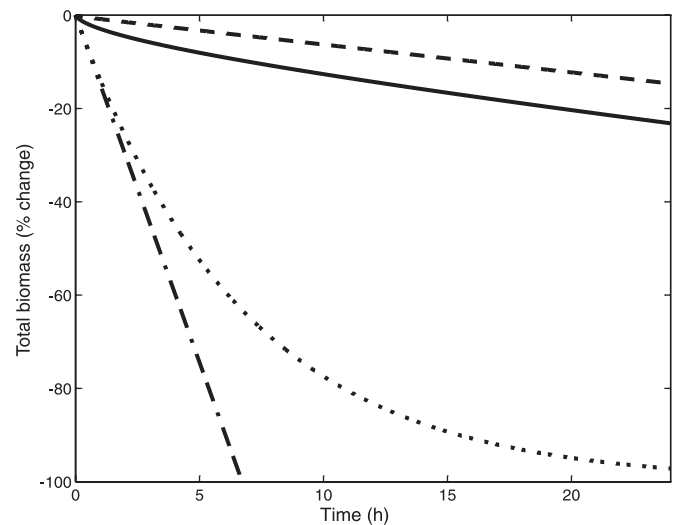


**Fig. 6.** Changes in total algal abundance computed from eq. 1 with parabolic eddy diffusivity distribution (solid line), eq. 1 with constant eddy diffusivity distribution (dashed line), well-mixed reactor model (dotted line), and no-refiltration model (dot-dashed line).



proaches (Fig. 6). Twenty-four-hour consumption estimates are 15% and 20% for solutions to eq. 1 (parabolic and uniform distribution of  $K$ , respectively) compared with 97% at 24 h for the well-mixed model and 100% at 6.8 h for the no-refiltration model. Vertical biomass distribution after 24 h varies owing to both the magnitude and shape of the diffusivity distribution with depth (Fig. 7). The parabolic shape induced less algal clearance than did the uniform distribution with the same depth-averaged diffusivity. Lower values of diffusivity resulted in declining algae near the sur-

**Fig. 7.** Simulated biomass profiles after 24 h versus height above bed ( $z$ ): solid line, parabolic eddy diffusivity with a mean of  $10^{-4} \text{ m}^2\cdot\text{s}^{-1}$ ; dot-dot-dashed line, uniform eddy diffusivity of  $10^{-4} \text{ m}^2\cdot\text{s}^{-1}$ ; dotted line, parabolic eddy diffusivity with a mean of  $10^{-5} \text{ m}^2\cdot\text{s}^{-1}$ ; dot-dashed line, uniform eddy diffusivity of  $10^{-5} \text{ m}^2\cdot\text{s}^{-1}$ .

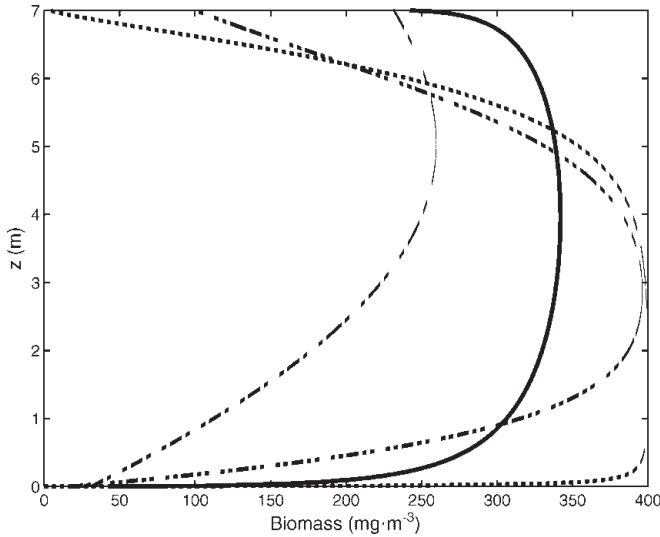
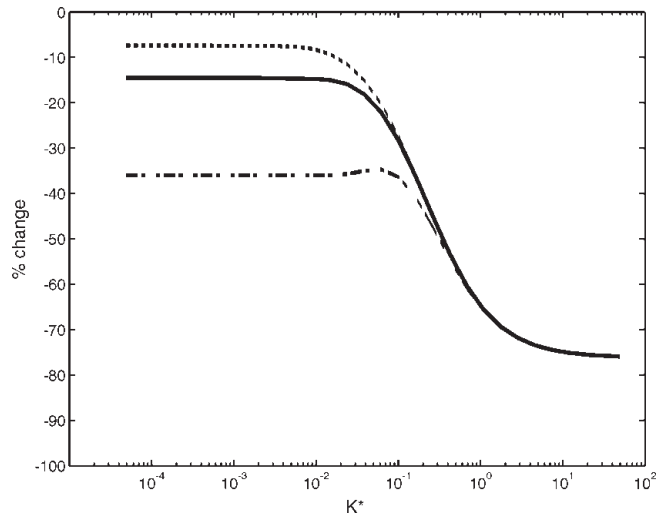


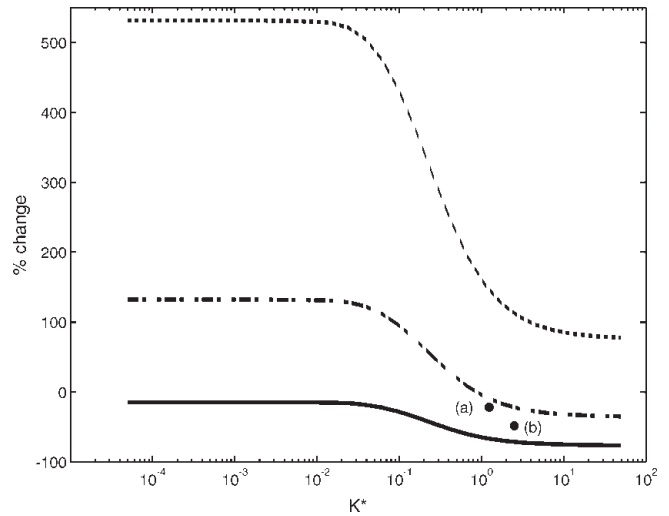
**Fig. 8.** Effect of mixing, expressed as a nondimensional diffusion coefficient ( $K^*$ ), on the predicted percent change in total algal abundance over 24 h for three values of the nondimensional sinking rate ( $w_s^*$ ): dotted line,  $w_s^* = 0.02$ ; solid line,  $w_s^* = 0.04$ ; dot-dash-dotted line,  $w_s^* = 0.1$ . The base values of  $\alpha$  and  $H$  (zebra mussel clearance rate and water depth, respectively) were used and  $K$  was varied between  $10^{-7}$  and  $10^{-1} \text{ m}^2\cdot\text{s}^{-1}$ .



face and very strong gradient of algal concentration near the bed.

Increases in the nondimensional sinking rate  $w_s^*$  result in increased depletion, except at high values of  $K^*$  (Fig. 8). Inclusion of phytoplankton production results in increased algal abundance relative to estimates without production (Fig. 9). High production has the greatest impact at low values of  $K^*$ , while there is increased clearance at all levels of production at high  $K^*$ .

**Fig. 9.** Effect of mixing and production, expressed in nondimensional terms, on the predicted percent change in total algal abundance over 24 h with varying nondimensional algal production ( $\mu^*$ ): solid line,  $\mu^* = 0$ ; dot-dash-dotted line,  $\mu^* = 0.28$ ; dotted line,  $\mu^* = 0.56$ . Markers indicate values calculated from Cloern (1991) (a) and Ackerman (2001) (b). The base values of  $\alpha$ ,  $w_s$ , and  $H$  (zebra mussel clearance rate, algal sinking rate, and water depth) were used and  $K$  was varied between  $10^{-7}$  and  $10^{-1} \text{ m}^2\cdot\text{s}^{-1}$ .



## Discussion

### Comparison with previous field measurements

These Lake Erie results are consistent with those from previous physical studies. We found that the power spectrum of horizontal velocities (at 1 m above bed) for the period of 10 June 1995 to 23 June 1995 corresponded to those found by Hamblin (1987) for the Lake Erie weather cycle (96 h), the first-mode seiches (14 h), the second-mode seiches (9 h), the third-mode seiches (6 h), and the cross-basin seiche (3 h). The second-mode seiches (9 h) are comparatively weak, as the sample site was very close to the second-mode node. A diel (24-h) signal was absent because the sampling captured only the influence of bed shear and could not detect convective events or diel thermocline formation because these do not influence horizontal currents. With this one exception, our results from a 5-m-deep near shore site have water currents characteristic of both the western basin and shallow regions of the lake as a whole. Thus, they can be used to study the effects of shear on grazing by zebra mussels.

Royer et al. (1987) found current velocities in the lake to vary from 1 to 10  $\text{cm}\cdot\text{s}^{-1}$  using several measuring methods, while Bedford and Abdelrhman (1987) predicted velocities of 1–5  $\text{cm}\cdot\text{s}^{-1}$  during calm weather and 10–20  $\text{cm}\cdot\text{s}^{-1}$  during storm events, both comparing favorably with our results. Shear velocities were slightly less than expected for our exposed site, varying from 0.13 to 1.66  $\text{cm}\cdot\text{s}^{-1}$ , almost one order of magnitude less than those predicted by Bedford and Abdelrhman (1987). However, the estimates of  $z_0$  were higher than they predicted, perhaps because of the zebra mussel covered cobbles. Although the cobbles were on the order of 8–10 cm, the mussel druses (large clumps of zebra

mussels) increased the size of the roughness elements to 20–30 cm or greater.

The magnitude of eddy diffusivities varied from  $10^{-5}$  to  $10^{-4} \text{ m}^2\cdot\text{s}^{-1}$ , with the largest values corresponding roughly to wind direction owing to the location of the sample site on the north side of an island. These values are consistently two orders of magnitude below the high diffusivities generated by tidal flows in shallow marine systems (on the order of  $10^{-2} \text{ m}^2\cdot\text{s}^{-1}$ ). Storm events in Lake Erie's much deeper central basin have been found to support diffusivities as high as  $10^{-2} \text{ m}^2\cdot\text{s}^{-1}$  (McCune 1998). That we did not obtain values this high in western Lake Erie was due, at least in part, to daily averaging of current speeds that, while more representative of conditions on the lake, could not capture short-term, high-intensity events such as severe storms. Storm events may be ecologically less important than less intense mixing events, since they can overwhelm the mussel filtering capacity; a large suspended sediment load causes the mussels to stop filtering (Ackerman 1999).

### Mussel impacts on algae

We found a strong zone of depletion in algal biomass from samples near the benthos in early and midsummer. The mussels were able to consume much of the algae in the near-bed region, causing a zone of depletion similar to that found by MacIsaac et al. (1999). However, the algal abundance and composition of the upper water column remained similar to those found prior to the introduction of the zebra mussel (Wu and Culver 1991). In late August and into September, there was increased biomass (dominated by the cyanobacterium *Microcystis*) near the benthos, as opposed to a zone of depletion.

The trend in algal vertical distribution observed in August and September 1995, an increase in algal biomass above the mussels, may be explained by the resurgence of the toxic cyanobacterium *Microcystis*. A large bloom of *Microcystis* first appeared in August 1995 (Culver et al. 1999). Various researchers (Heath et al. 1995; Holland et al. 1995; Arnott and Vanni 1996) have attributed such blooms, including a subsequent bloom in 1998, to the excretion of nitrogen and phosphorus by zebra mussels. However, while *Microcystis* is therefore an integral part of the zebra mussel problem, it has two qualities that cause it to interfere with estimates of the impacts of the zebra mussels on the phytoplankton community: first, it migrates vertically to obtain the best light and nutrient regimens, and second, large colonies are rejected by zebra mussels and may reenter the water column (Vanderploeg et al. 2001). Thus the phytoplankton maximum observed herein may be then a product of both the alga's migration ( $w_s \neq 1$ ) and the zebra mussels' preference not to consume it.

While we observed little evidence of algal depletion away from the benthos, others have estimated much greater consumption of algae from the whole water column by the zebra mussels based on filtering estimates (MacIsaac et al. 1992, 1999; Bunt et al. 1993) and bioenergetic models (Madenjian 1995). Their estimates of clearance rates (cubic metres per square metre per day) indicate that a volume equivalent to that of the entire water column can theoretically be filtered completely once per day by small-bodied individuals (Bunt et al. 1993) and between 3.5 and 18.8 times per day by the

whole community (MacIsaac et al. 1992). However, it has been unclear how close to the theoretical maximum filtering (pumping) rate the mussel community actually achieves and what fraction of the algae in the water column is consumed per day. Yu and Culver (1999) found that refiltration of water previously cleared of algae can significantly decrease the mussels' impact on the algal population, while Hogan and Mills (1997) correspondingly observed decreased clearance rates as algal concentrations decreased.

### Effects of finite mixing

We compared the algal consumption predicted by the no-refiltration model of MacIsaac et al. (1992) and others, the well-mixed reactor model, and the finite-mixing model. The solution of eq. 1 used  $\mu = 0$  as in the two simpler models, an initially uniform algal concentration, and constant and parabolic eddy diffusivity distributions with a depth-averaged diffusivity of  $10^{-4} \text{ m}^2\cdot\text{s}^{-1}$ , which is an upper bound on the average diffusivities measured in the field. The western basin of Lake Erie is not well mixed, so when the vertical mixing is finite, the predicted algal clearance determined by eq. 1 is much less than that from either the no-refiltration or the well-mixed model. Only 2% of the algae is removed from the lake (assuming a parabolic diffusivity distribution) after 6.8 h, when the no-refiltration model predicts that the algae have been completely filtered from the lake. After a day, the well-mixed model predicts that 97% of the algae have been consumed, while the solution of eq. 1 gives only 15% and 20% of the algae removed per day for depth-averaged eddy diffusivities of  $10^{-5}$  and  $10^{-4} \text{ m}^2\cdot\text{s}^{-1}$ . The values from the model with no-refiltration are similar to the  $26 \pm 10\%$  predicted by Madenjian's (1995) bioenergetic approach. However, shallow waters will be affected more severely by the mussels' filtering ability. Reducing the water column height from 7 to 2 m causes the consumption results of eq. 1 to jump to 47% and 80% for  $K = 10^{-5}$  and  $10^{-4} \text{ m}^2\cdot\text{s}^{-1}$ , respectively. This result is consistent with other nearshore field research including changes in nearshore algal communities (Hatchery Bay, Lake Erie; Holland et al. 1995) and benthic invertebrates (Saginaw Bay, Lake Michigan; Nalepa et al. 2003).

The vertical distribution of the eddy diffusivity strongly affects the changes in the algal profiles over 24 h and hence the estimates of grazing rates by zebra mussels. The shape of the eddy diffusivity profile is important because the lower diffusivity near the bottom in the parabolic profile reduces algal transport to the benthos. When the eddy diffusivity is uniform over the depth, the consumption increases; clearance rates for the uniform diffusivity distribution after 24 h are 49% and 23% for eddy diffusivities of  $10^{-4}$  and  $10^{-5} \text{ m}^2\cdot\text{s}^{-1}$ , respectively. In addition, lower diffusivities near the bottom lead to very thin layers of algal depletion, and near the water surface, the mixing is too weak to counteract sinking.

### Effect of time scales

Using the three dimensionless parameters, we systematically examined the effects of diffusivity, sinking rate, and algal reproduction rate. As the eddy diffusivity increases, the consumption rate increases for all values of sinking rate. At low  $K^*$ , sinking controls consumption, while at higher  $K^*$ , mixing controls consumption. In particular, for  $K^* > 0.3$ , the

sinking rate is unimportant. When  $K^* > 10$ , the consumption no longer depends on  $K$ , and if a uniform eddy diffusivity profile were used, the clearance would be  $97\% \cdot \text{day}^{-1}$  as in the well-mixed model. These results allow “well mixed” to be defined quantitatively. For example, for the western basin of Lake Erie to be well mixed, the eddy diffusivity would have to exceed  $2 \times 10^{-2} \text{ m}^2 \cdot \text{s}^{-1}$ , which is more than 100 times higher than our measured values. In addition, for the same  $K$  and  $\alpha$ , a reduced depth increases  $K^*$ , resulting in greater algal clearance.

However, these estimates and our previous comparison with other works lack a fundamental part of the algal transport process and consumption dynamic: algal production. When we include productivity, we can compare our work with previous effort in other systems and even calculate values for  $K^*$  and  $\mu^*$  from their data. Cloern (1991) first used a similar model in a marine tidal system with parabolic diffusivity profiles ( $K = 5 \times 10^{-5} \text{ m}^2 \cdot \text{s}^{-1}$  and  $K^* = 0.625$ ) and found algal removal rates of  $6.3\% \cdot \text{day}^{-1}$ . Increasing mixing by one order of magnitude increased consumption to  $33\% \cdot \text{day}^{-1}$ . His results include an algal source term, resulting in decreased clearing at low  $K^*$ . Ackerman et al. (2001) investigated the impacts of grazing across a single dreissenid mussel bed in western Lake Erie, estimating clearance from the beginning to the end of the bed in addition to physical parameters. At  $K^* = 1.25$ , they found 40% algal clearance across the bed, although without a source term. We find that our estimates of algal consumption are similar but diverge with increasing production. Higher production values and decreased mixing ( $K^*$ ) can result in rapid increases in algal population, especially as the higher productivity regions (near the surface) are separated in space from mussel consumption. With high  $\mu$  ( $\mu^* = 0.56$ ) and high  $K^*$ , the increase becomes less profound, as the mussels have access to more of the water through increased mixing. Low productivity,  $\mu^* = 0$ , results in increasing depletion of the water column with that depletion strongly linked to mixing,  $K^*$ . Less extreme values in productivity,  $\mu^* = 0.28$  (equivalent to one algal replication per day), result in modest increases or decreases, depending on the intensity of the mixing. This result appears most reasonable, given the lack of evidence for changes in seasonal algal abundance patterns in the lake since dreissenids became established (Wu and Culver 1991).

In summary, a series of field experiments in a nearshore region of Lake Erie produced diffusivity estimates that did not exceed  $10^{-4} \text{ m}^2 \cdot \text{s}^{-1}$  (averaged over 24-h periods) despite small storm events. Because of the relatively weak mixing, the strong dependence of benthic feeding rates on hydrodynamic processes that has been consistently observed in the marine literature is even more important in large lakes. Modeled algal depletion was strongly linked to the magnitude and shape of the diffusivity profile, indicating both that the no-refiltration and well-mixed reactor models for estimating algal consumption grossly overestimate zebra mussel consumption and that there is a strong need for research into the shape of the diffusivity profiles in large lakes. Vertical algal profiles taken during the sampling verify that algal depletion is strongly influenced by hydrodynamic forcing. Finally, future efforts to estimate the impact of the benthos on the planktonic algal community must be linked to estimates of algal productivity and hydrodynamic forcing.

## Acknowledgements

We thank the National Science Foundation for the funding for this project (NSF award 9503170). We also thank Karen Mather and Angie Gingerich for their help with phytoplankton enumeration and other assistance and John Hageman and Jeffrey Reutter at the F.T. Stone Laboratory, Ohio State University. The research was partially funded by the Federal Aid in Sport Fish Restoration Program (F-69-P, Fish Management in Ohio), administered jointly by the US Fish and Wildlife Service and the Ohio Division of Wildlife.

## References

- Ackerman, J.D. 1999. Effect of velocity on the filter feeding of dreissenid mussels (*Dreissena polymorpha* and *Dreissena bugensis*): implications for trophic dynamics. *Can. J. Fish. Aquat. Sci.* **56**: 1551–1561.
- Ackerman, J.D., Loewen, M.R., and Hamblin, P.F. 2001. Benthic–pelagic coupling over a zebra mussel bed in the western basin of Lake Erie. *Limnol. Oceanogr.* **46**: 892–904.
- Arnott, D.L., and Vanni, M.J. 1996. Nitrogen and phosphorus recycling by the zebra mussel (*Dreissena polymorpha*) in the western basin of Lake Erie. *Can. J. Fish. Aquat. Sci.* **53**: 646–659.
- Bedford, K.W., and Abdelrhman, M. 1987. Analytical and experimental studies of the benthic boundary layer and their applicability to near-bottom transport in Lake Erie. *J. Gt. Lakes Res.* **13**: 628–648.
- Bunt, C.M., MacIsaac, H.J., and Sprules, W.G. 1993. Pumping rates and projected filtering impacts of juvenile zebra mussels (*Dreissena polymorpha*) in western Lake Erie. *Can. J. Fish. Aquat. Sci.* **50**: 1017–1022.
- Chriss, T.M., and Caldwell, D.R. 1982. Evidence for the influence of form drag on bottom boundary layer flow. *J. Geophys. Res.* **87**: 4148–4154.
- Cloern, J.E. 1991. Tidal stirring and phytoplankton bloom dynamics in an estuary. *J. Mar. Res.* **49**: 203–221.
- Culver, D., Li, H., and Babcock-Jackson, L. 1999. Lake Erie phytoplankton at the millennium: nutrients, zebra mussels, and the future. Invited paper for the Lake Erie Millennium Conference, 26–28 April 1999. University of Windsor, Windsor, Ont.
- Douglas, J. 1961. A survey of numerical methods for parabolic differential equations. *In Advances in computers. Version 2. Edited by F. Alt.* Academic Press, New York. pp. 1–54.
- Fischer, H.B., List, E.J., Koh, R.C.Y., Imberger, J., and Brooks, N.H. 1979. Mixing in inland and coastal waters. Academic Press, New York.
- Frechette, M., and Bourget, E. 1985a. Energy flow between the pelagic and benthic zones: factors controlling particulate organic matter available to an intertidal mussel bed. *Can. J. Fish. Aquat. Sci.* **42**: 1158–1165.
- Frechette, M., and Bourget, E. 1985b. Food-limited growth of *Mytilus edulis* L. in relation to the benthic boundary layer. *Can. J. Fish. Aquat. Sci.* **42**: 1166–1170.
- Frechette, M., Butman, C.A., and Geyer, W.R. 1989. The importance of boundary-layer flow processes in supplying phytoplankton to the benthic filter feeder, *Mytilus edulis*. *Limnol. Oceanogr.* **34**: 19–36.
- Hamblin, P.F. 1987. Meteorological forcing and water level fluctuations of Lake Erie. *J. Gt. Lakes Res.* **13**: 436–453.
- Heath, R.T., Fahnensteil, G., Gardner, W.S., Cavaletto, J.F., and Hwang, S.J. 1995. Ecosystem level effects of zebra mussels *Dreissena polymorpha*: an enclosure experiment in Saginaw Bay. *J. Gt. Lakes Res.* **21**: 501–516.

- Hinze, J.O. 1975. Turbulence. 2nd ed. McGraw-Hill, New York.
- Hogan, M.J., and Mills, E.L. 1997. Clearance rates and filtering activity of zebra mussel (*Dreissena polymorpha*): implications for freshwater lakes. *Can. J. Fish. Aquat. Sci.* **54**: 249–255.
- Holland, R.E., Johengen, T.H., and Beeton, A.M. 1995. Trends in nutrient concentrations in Hatchery Bay, western Lake Erie, before and after *Dreissena polymorpha*. *Can. J. Fish. Aquat. Sci.* **52**: 1202–1209.
- Hutchinson, G.E. 1967. A treatise on limnology. Wiley, New York.
- James, W.F., Barko, J.W., and Eakin, H.L. 1997. Nutrient regeneration by the zebra mussel (*Dreissena polymorpha*). *J. Freshw. Ecol.* **12**: 209–216.
- Jumars, P.A., and Nowell, A.R.M. 1984. Fluid and sediment dynamic effects on marine benthic community structure. *Am. Zool.* **24**: 45–55.
- Kelly, J.G.W., Hobgood, J.S., Bedford, K.W., and Schwab, D.J. 1998. Generation of three-dimensional lake model forecasts for Lake Erie. *Weather Forecast.* **13**: 659–687.
- Koseff, J.R., Holen, J.K., Monismith, S.G., and Cloern, J.E. 1993. Coupled effects of vertical mixing and benthic grazing on phytoplankton populations in shallow, turbid estuaries. *J. Mar. Res.* **51**: 843–868.
- Lucas, L.V., Koseff, J.R., Cloern, J.E., Monismith, S.G., and Thompson, J.K. 1999. Processes governing phytoplankton blooms in estuaries I: The local production–loss balance. *Mar. Ecol. Prog. Ser.* **187**: 1–15.
- MacIsaac, H.J., Sprules, W.G., Johannsson, O.J., and Leach, J.H. 1992. Filtering impact of larval and sessile zebra mussels (*Dreissena polymorpha*) in western Lake Erie. *Oecologia*, **92**: 30–39.
- MacIsaac, H.J., Johannsson, O.J., Ye, J., Leach, J.H., McCorquodale, J.A., and Grigorovich, I.A. 1999. Filtering impacts of and introduced bivalve (*Dreissena polymorpha*) in a shallow lake: application of a hydrodynamic model. *Ecosystems*, **2**: 338–350.
- Madenjian, C.P. 1995. Removal of algae by the zebra mussel (*Dreissena polymorpha*) population in western Lake Erie — a bioenergetics approach. *Can. J. Fish. Aquat. Sci.* **52**: 381–390.
- Makarewicz, J.C., Lewis, T., and Bertram, P. 1999. Phytoplankton composition and biomass in the offshore waters of Lake Erie: pre- and post-*Dreissena* introduction. *J. Gt. Lakes Res.* **25**: 135–148.
- McCune, K. 1998. Temperature gradient microprofiling in the central basin of Lake Erie: a study of vertical turbulent processes. M.S. thesis, Ohio State University, Columbus.
- Monismith, S.G., Koseff, J.R., Thompson, J., O’Riordan, C.A., and Nepf, H.M. 1990. A study of model bivalve siphonal currents. *Limnol. Oceanogr.* **35**: 680–696.
- Muschenheim, D.K. 1987. The dynamics of near-bed seston flux and suspension-feeding benthos. *J. Mar. Res.* **45**: 473–496.
- Nalepa, T.F., Fanslow, D.L., Lansing, M.B., and Lang, G.A. 2003. Trends in the benthic macroinvertebrate community of Saginaw Bay, Lake Huron, 1987 to 1996: responses to phosphorus abatement and the zebra mussel, *Dreissena polymorpha*. *J. Gt. Lakes Res.* **29**: 14–33.
- Peterson, C.H., and Beal, B.F. 1989. Bivalve growth and higher order interactions: importance of density, site and time. *Ecology*, **70**: 1390–1404.
- Peterson, C.H., and Black, R. 1987. Resource depletion by active suspension feeders on tidal flats: influence of local density and tidal elevation. *Limnol. Oceanogr.* **32**: 143–166.
- Pontius, R.A., and Culver, D.A. 2001. Estimating zebra mussel impact on pelagic food webs: the role of size-specific grazing rates. *Verh. Int. Ver. Limnol.* **27**: 3025–3028.
- Royer, L., Hamblin, P.F., and Boyce, F.M. 1987. A comparison of drogues, current meters, winds and a vertical profiler in Lake Erie. *J. Gt. Lakes Res.* **13**: 578–586.
- Vanderploeg, H.A., Liebig, J.R., Carmichael, W.W., Agy, M.A., Johengen, T.H., Fahnenstiel, G.L., and Nalepa, T.F. 2001. Zebra mussel (*Dreissena polymorpha*) selective filtration promoted toxic *Microcystis* blooms in Saginaw Bay (Lake Huron) and Lake Erie. *Can. J. Fish. Aquat. Sci.* **58**: 1208–1221.
- Wildish, D.J., and Kristmanson, D.D. 1984. Importance of mussels of the benthic boundary layer. *Can. J. Fish. Aquat. Sci.* **41**: 1618–1625.
- Wright, R.R., Coffin, R.B., Ersing, C.P., and Pearson, D. 1982. Field and laboratory measurements of bivalve filtration of natural marine bacterioplankton. *Limnol. Oceanogr.* **27**: 91–98.
- Wu, L., and Culver, D.A. 1991. Zooplankton grazing and phytoplankton abundance: an assessment before and after invasion of *Dreissena polymorpha*. *J. Gt. Lakes Res.* **17**: 425–436.
- Yu, N., and Culver, D.A. 1999. Estimating the effective clearance rate and refiltration by zebra mussels, *Dreissena polymorpha*, in a stratified reservoir. *Freshw. Biol.* **41**: 481–492.